Conducted depolarization in arteriole networks of the guinea-pig small intestine: effect of branching on signal dissipation

Steven S. Segal* and Timothy O. Neild

Department of Human Physiology, Flinders University, GPO Box 2100, Adelaide 5001, Australia

with an Appendix by Timothy O. Neild

1. Blood flow control requires co-ordinated activity among many branches of arteriole networks, which may be achieved by conduction of membrane potential changes between arteriolar smooth muscle cells and endothelial cells.

2. We investigated the effect of branching upon the passive conduction of electrical signals through the syncytium of electrically coupled cells in arteriole networks ($n = 12$) prepared from the guinea-pig submucosa. To describe the effect of branching on cable properties, the expansion parameter B was calculated ($B = 1$ for an unbranched cable; $B > 1$ with branching) for a point in each arteriole network based on anatomy.

3. An estimate of $B(B')$ was also obtained by measuring the spread of depolarization caused by a high-K^+ stimulus applied to one region. Membrane potential (-74 ± 4 mV ($\pm$ S.D.) at rest) was recorded from smooth muscle cells (verified with intracellular dye labelling). A micropipette containing 120 mM KCl was positioned at 150 μm increments along an arteriole (width, 50–75 μm) up to ~1·2 mm from a stationary recording site, producing stable depolarization which decreased as separation distance increased. The dissipation of depolarization with separation was greater when recording near branch origins rather than continuous segments.

4. B ranged in value from 0·99 to 2·28. In any one experiment, values of B and B' were correlated (correlation coefficient, $r = 0·71$; $P < 0·05$), but B' was consistently greater than B, and we discuss methodological factors which could lead to erroneously high values for B'.

5. For pooled electrophysiological data, depolarization decayed to 37 % ($1/e$) of initial values in ~700 μm, consistent with $B > 1$. In contrast, the conduction of vasoconstriction and vasodilatation exceeds 2 mm in arteriole networks in previous studies. To explain this discrepancy, we suggest that active electrical events in cells of the arteriole wall augment passive electrical conduction during blood flow control.

The spread of vasomotor responses beyond the site directly affected by a stimulus was first shown in the frog microcirculation early this century (Krogh, Harrop & Rehberg, 1922). In 1970, microiontophoresis of acetylcholine was found to trigger the 'propagation' of dilatation along arterioles of the hamster cheek pouch for distances of several hundred micrometres beyond the stimulus site (Duling & Berne, 1970). Although these original studies of spreading and propagated vasomotor responses were taken to reflect neurally mediated mechanisms, more recent studies in hamster cremaster muscle and cheek pouch preparations have revealed an alternative mechanism for the transmission of signals throughout arteriole networks: direct cell-to-cell electrical coupling between the smooth muscle cells and endothelial cells which comprise the vascular wall (Segal & Duling, 1986; Segal, 1991; Segal & Bény, 1992; Bény & Pacicca, 1994; Little, Xia & Duling, 1995; Xia, Little & Duling, 1995).

The control of tissue blood flow requires a concerted interplay among the many branches of a resistance network. Direct coupling among the cells which control arteriolar diameter thereby provides a mechanism for rapidly co-ordinating vasomotor activity throughout the network

* To whom correspondence should be addressed at The John B. Pierce Laboratory, Yale University School of Medicine, 290 Congress Avenue, New Haven, CT 06519, USA.

(Segal & Duling, 1986; Segal, Damon & Duling, 1989; Segal, 1991). Conducted vasodilatation in arterioles is readily triggered using microiontophoresis of acetylcholine (Segal *et al.* 1989; Kurjiaka & Segal, 1995); the initial event appears to be the hyperpolarization of endothelial cells in response to muscarinic receptor activation (Olesen, Davies & Clapham, 1988; Chen & Cheung, 1992; Segal & Bény, 1992). The hyperpolarization has been proposed to spread passively from cell to cell along the arteriole wall, resulting in vasodilatation in proportion to the change in membrane potential (E_m) (Segal & Duling, 1989). In a complementary fashion, the conduction of vasoconstriction (Segal *et al.* 1989; Delashaw & Duling, 1991) reflects the triggering and spread of depolarization along the arteriole wall (Morgan, 1983; Hirst & Edwards, 1989; Xia & Duling, 1995). The amplitude of conducted responses in arterioles decays bidirectionally with distance from the stimulus site, which is in accord with the passive electrical properties of tissues in which cells are electrically coupled (Jack, Noble & Chen, 1975; Hirst & Neild, 1978; Neild, 1983), yet contrasts with regenerative activity inherent in neural propagation. Analogous to the passive spread of E_m changes, the decay of conducted vasomotor responses has been characterized by 'mechanical' length constants of ~ 2 mm (Segal & Duling, 1986; Segal *et al.* 1989; Segal, 1991), which describe the distance required for the vasomotor response to decline to 37% ($1/e$) of its initial value. Implicit in this analogy was the assumption that changes in diameter reflected the spread of electrical signals along the arteriole wall.

Both vasodilatation and vasoconstriction are conducted rapidly along arterioles over distances that encompass several millimetres and multiple branch orders (Segal *et al.* 1989; Segal, 1991). Intracellular dye microinjection has revealed pronounced gap-junctional coupling among cells of the arteriole wall (Segal & Bény, 1992; Little *et al.* 1995). Further, antagonists of gap junctions reversibly impair conducted vasomotor responses (Segal & Duling, 1989). Thus, an increasing body of evidence supports the hypothesis that cell-to-cell coupling provides the pathway for conduction.

The original studies of electrical conduction in arterioles were performed on arterioles of the guinea-pig submucosa (Hirst & Neild, 1978). To avoid the complications due to branching, arteriole segments were prepared using microdissection to obtain isolated 'cables'. In so doing, the first electrophysiological measurements of the length constant (λ) for the passive spread of depolarization in arterioles were obtained. Whereas λ is the exponential constant for electrical spread in an unbranched cable, the changes in E_m throughout a branching network should have a more complicated dependence on λ due to the additional paths for current flow (Jack *et al.* 1975). However, there is a paucity of information concerning the influence of branching on the spread of electrical signals in arteriole networks, and the magnitude of this effect is unknown. The purpose of this study was to investigate the effect of branching on the conduction of depolarization in arteriole networks and develop a quantitative description of this behaviour using cable theory.

When a cable branches (or expands), the electrical properties of the network can be described using an expansion factor B, which indicates how the branched region differs in input conductance from a uniform infinite cable (Jack *et al.* 1975, p. 32). If B has a value of 1 the network has the same DC electrical characteristics as the arteriole from which it branches. Values of B greater than 1 imply expansion (branching) of the network, with greater dissipation of an electrical signal into contiguous branches. In order to calculate what the change in E_m will be in an arteriole network in response to a stimulus at another point, we need to know the cable properties of the vessels and the value of B. In this paper we present a calculation of B based upon the anatomy of the arteriolar network and compare it with values estimated from electrophysiological measurements of the spread of depolarization.

METHODS

Tissue preparation

Guinea-pigs of either sex (Institute of Medical and Veterinary Science outbred strain, 200–300 g) were obtained from the Flinders University Animal House. On the day of an experiment, a guinea-pig was killed by a heavy blow to the head and exsanguinated, using procedures approved by the Flinders University Animal Welfare Committee. A 10–15 cm length of ileum was excised and placed in a beaker of physiological saline solution (PSS) of the following composition (in mmol l^{-1}): Na$^+$, 146; K$^+$, 5; Ca^{2+}, 2·5; Mg^{2+}, 2; Cl$^-$, 134; HCO$_3^-$, 25; H$_2$PO$_4^-$, 1; and glucose, 11; the PSS was equilibrated with 95% O$_2$–5% CO$_2$ (pH 7·4). The tissue was immersed in fresh PSS throughout dissection, which was done at room temperature (23–25 °C). Using an Olympus SZ40 stereo microscope, a 1–2 cm segment of ileum containing microvascular trees was dissected as a ring, then opened into a strip. The tissue was pinned to the bottom of a Petri dish covered with Sylgard (Dow Corning) and the mucosa was carefully peeled away using fine surgical forceps to expose the submucosal connective tissue layer which contained arteriole and venule networks. A piece of submucosal connective tissue (10 mm × 10 mm) containing at least one vascular tree was dissected free and pinned into a circular chamber (23 mm diameter, 1 mm deep) contained in a circular platform (50 mm diameter, 5 mm thick).

Instrumentation

The platform containing the submucosa preparation was secured on the stage of an inverted microscope (Leitz Diavert) and superfused continuously at 5 ml min^{-1} with PSS maintained at 37 °C; the direction of PSS flow across the preparation was directed perpendicularly to experimental sites by rotating the platform to the appropriate position. The preparation was transilluminated with unfocused light from a 100 W halogen lamp through a green filter (535–560 nm bandwidth) to facilitate resolution of the arteriole wall. The preparation equilibrated for 1 h before experimentation; during this time a sketch of the network was made while viewing the preparation at × 40 magnification using a × 4 objective. For intracellular recording, arterioles were viewed at a final magnification of × 100 using a × 10 objective (numerical aperture, 0·25). Electrophysiological data were acquired at 500 Hz

on a 386 personal computer using an A/D interface (DT100; Axon Instruments, Foster City, CA, USA) and AxoTape software (version 2.0; Axon Instruments). Resting and response values for E_m were obtained from AxoTape records of membrane tagged to correspond with separation distance between the high-K^+ stimulus pipette and the intracellular microelectrode (detailed below).

Intracellular recording

Borosilicate glass capillary tubing (1·0 mm o.d. × 0·58 mm i.d.; Clark Electromedical Instruments, Pangbourne, Berks, UK) was pulled (Flaming Brown model P-87 pipette puller; Sutter Instruments, Novato, CA, USA) to form microelectrodes which, when filled with 2 M KCl, had resistances of 100–200 MΩ. After mounting in a micromanipulator (Leitz model M), a silver wire connected the microelectrode to the headstage of the amplifier (model 1600; A-M Systems, Everett, WA, USA); a second silver wire secured at the edge of the chamber served as the reference electrode.

For penetration with microelectrodes, arterioles were approached vertically from above, increasing the likelihood of impaling a smooth muscle cell before an endothelial cell (Rhodin, 1967; Hirst & Neild, 1978; Segal & Bény, 1992). The acceptance of electro-physiological data was based upon satisfying several criteria: (i) the clean penetration of a cell, demonstrated by a rapid drop in potential from zero; (ii) a stable resting E_m for at least 3 min; (iii) a E_m of at least −60 mV; and (iv) a clean exit from the cell, demonstrated by a rapid return to zero potential. Microelectrodes were positioned in the centre of the arteriole as, with contraction, the vessel edges moved towards the centre line, where displacement was minimal. In the successful experiments, which form the electrophysiological basis of this study, stable recordings lasted for 5–20 min.

In additional experiments, the exact cellular location of intra-cellular recording sites was ascertained by microinjecting Lucifer Yellow dye (dilithium, MW 457; Molecular Probes) using glass microelectrodes of identical configuration to those used for recording. Using fine glass capillary tubing (o.d., 450 μm; Polymicro Technologies, Phoenix, AZ, USA), the electrode tip was backfilled with Lucifer Yellow prepared as a 4% (81 mM) solution in distilled deionized water, with the remainder filled with 150 mM LiCl (Segal & Bény, 1992); filling solutions were filtered to remove particles > 0·2 μm (Acrodisc; Gelman, Ann Arbor, MI, USA). The resistance of these microelectrodes was typically 400–600 MΩ.

High-potassium micropipettes

Micropipettes (tip i.d., 10–25 μm) were filled with PSS containing 120 mmol l⁻¹ KCl (referred to as 'high K^+'), prepared by replacing 115 mmol l⁻¹ of NaCl with KCl. A high-K^+ micropipette was positioned with the tip located 5–10 μm above the arteriole surface using a Narishige micromanipulator (model MN-151). When not located on the arteriole, the high-K^+ pipette was positioned 150–200 μm away from the vessel in the downstream of PSS flow. As confirmed visually and by the lack of vasomotor response to acetylcholine (Sigma; 1 mmol l⁻¹ applied via micropipette), arterioles had low resting tone and remained dilated until the KCl pipette was positioned above the arteriole, at which time a brisk vasoconstriction was observed. Passive leak from the high-K^+ pipette was assumed to establish a raised extracellular K^+ concentration for the vessel segment below the pipette tip, resulting in smooth muscle cell depolarization. Judicious positioning of the high-K^+ pipette relative to the direction of superfusate flow ensured that KCl leak was directed perpendicularly to the vessel and away from the application site; rotation of the chamber platform and repositioning the high-K^+ pipette was used to achieve this condition. Control experiments with similar micropipettes

containing Evans Blue dye (ICN Pharmaceuticals, Costa Mesa, CA, USA) confirmed this behaviour of effluent from the micropipette tip. During a stable response, it was typical to see maximal vaso-constriction (i.e. complete or near closure of the lumen) of the segment directly in the path of the high-K^+ pipette within 2 s of stimulation; this response was useful for verifying the efficacy of high-K^+ stimulation at a specific site. We interpret these experimental conditions as the direct presentation of a depolarizing K^+ stimulus to an arteriole segment whose length was 1–2 times the vessel width (typically 50–70 μm) of the stimulated segment. This consideration implies that vasoconstriction beyond a distance of ∼150 μm on either side of the pipette tip does not represent a diffusion gradient for KCl; rather, it reflects the conduction of vaso-constriction from the stimulus origin (Segal *et al.* 1989).

Data analysis

All calculations were performed using a spreadsheet program (Microsoft Excel, version 4.0) on a 486 personal computer. Curve fitting was performed using the program's optimization routine which was based on a Marquardt procedure. The fit of each curve was verified by restarting the procedure with different sets of initial values of the free parameters and ascertaining that a unique fit was obtained for each set of starting values.

RESULTS

Determination of *B* from network anatomy

Values of *B* were calculated for a defined point in each of ten arteriolar networks, using refinements of the analysis and equations used previously to describe the branching of dendritic trees (see Appendix). In essence, this approach provides an index for predicting the effect of the anatomy of the network on its electrophysiological properties during electrical conduction. The spread of depolarization in each network was also measured, as described in the next section. Using a calibrated reticle in the eyepiece of the microscope, the length and diameter of the arteriole segments influencing *B* were carefully measured for up to eight branch orders beyond the recording site; the network was then redrawn in the form of a binary tree (Fig. 1). When a vessel changed diameter without branching it was represented as a branch point, with one branch having measured dimensions and another with zero diameter. In these preparations, small arteriolar branches terminate where they leave the submucosal layer and enter the mucosa, which was removed during dissection. In accordance with the observations of Hirst & Neild (1978), we have assumed that these terminating branches were electrically sealed and assigned them a value of 0 for *B*, and we have taken a value of 1·2 mm for the space constant (λ). Arteriole wall thickness was taken as 3·3 μm (Hua & Cragg, 1980).

As determined empirically, data from successive branch orders were included for each network until *B* changed by less than 0·1 units with inclusion of subsequent branches. In practice, *B* for a point in a segment which continued without branching for more than about 300 μm required the inclusion of data for only one or two subsequent branch orders, attributable to the continuous 'cable' being a principle determinant of current flow. In contrast, when

dealing with points near regions of extensive branching, four to eight branch orders were included to account for the multiple paths of signal dissipation.

Our results for the anatomical determinations of B ranged from 1·0 to 2·3 and are summarized in Fig. 3, where they are compared with values from electrophysiological experiments on the same arteriole networks.

Electrophysiological estimation of B

Stable, continuous recordings were obtained from cells in twelve arteriole networks. With the recording site constant, the high-K^+ pipette was positioned in increments of $\sim$150 μm along the principal branch under study for distances of up to $\sim$1200 μm from the microelectrode (Fig. 2); this distance encompassed the optical field of view using the $\times$10 objective. Whenever the high-K^+ pipette was positioned over the arteriole, the vessel lumen under the pipette constricted maximally (i.e. to near closure) within 1–2 s; this vasoconstriction declined along a distance of 250–300 μm on either side of the K^+ pipette and was sustained for the duration of the stimulus, which was

typically 6–10 s. In three experiments, recordings were maintained when the high-K^+ solution was applied directly at the recording site despite the accompanying vasoconstriction.

For each stimulus site, E_m was recorded at rest with the high-K^+ pipette removed from the vessel and then monitored continuously throughout the depolarizing stimulus (Fig. 2). The response data were expressed, with respect to separation distance, as the amplitude of depolarization (mV); this was calculated as: (E_m during depolarization plateau) $-$ (E_m at rest prior to high-K^+ stimulus). In several experiments, the high-K^+ stimulus was reapplied to the same sites after stimulating at other locations and the same magnitude of constriction and depolarization were observed (data not shown). These findings verify that the high-K^+ stimulus was constant, reproducible, and that a stable depolarization gradient was induced along the arteriole wall.

The K^+ would also have reached the perivascular nerves and might have excited them, but we think this was unlikely for
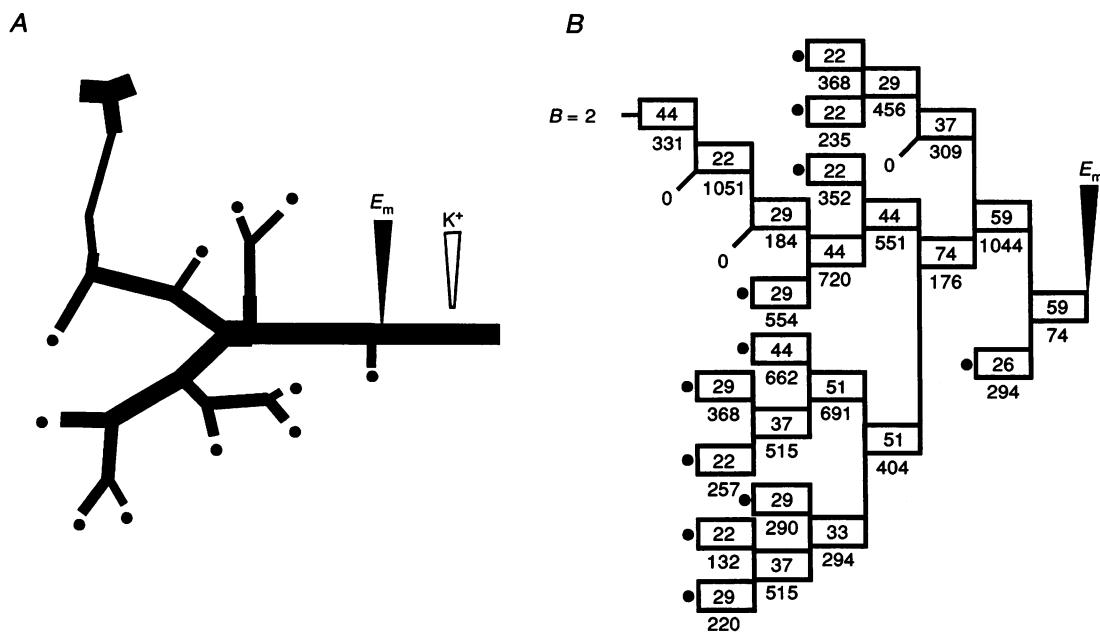
Figure 1. Anatomical determination of the expansion parameter B

A, line drawing (approximately to scale) of part of an arteriolar tree in an isolated preparation of the guinea-pig submucosa. A recording electrode (filled tip) and high-K^+ pipette are shown in the positions used to obtain the data shown in Fig. 2. Because the recording site is fixed and the stimulus applied to an uninterrupted segment to the right of the electrode, the dissipation of depolarization is determined by the cumulative cable properties of the branching network to the left of the electrode, the anatomy of which is redrawn in *B*. *B*, binary tree of network anatomy. Within each box is the width of the arteriole segment; below each box is the corresponding segment length. For example, to the left of the electrode, the parent vessel (width, 59 μm) continued for 74 μm and gave rise to a branch (width, 26 μm; length 294 μm), then continued at 59 μm for another 1044 μm. Filled circles at the end of branches indicate terminations where branches were sealed during dissection, thereby forming electrically open-circuit terminations (Hirst & Neild, 1978). A branch of '0' was used when a segment changed diameter without branching. The connection to an adjacent tree via the small branch in upper left of *A* (diameter, 44 μm; length, 331 μm) was accounted for by assigning $B = 2$ to the large 'T' to which it connects. Doubling or halving this assumed value changed the calculated B for the network by <0·003 %.
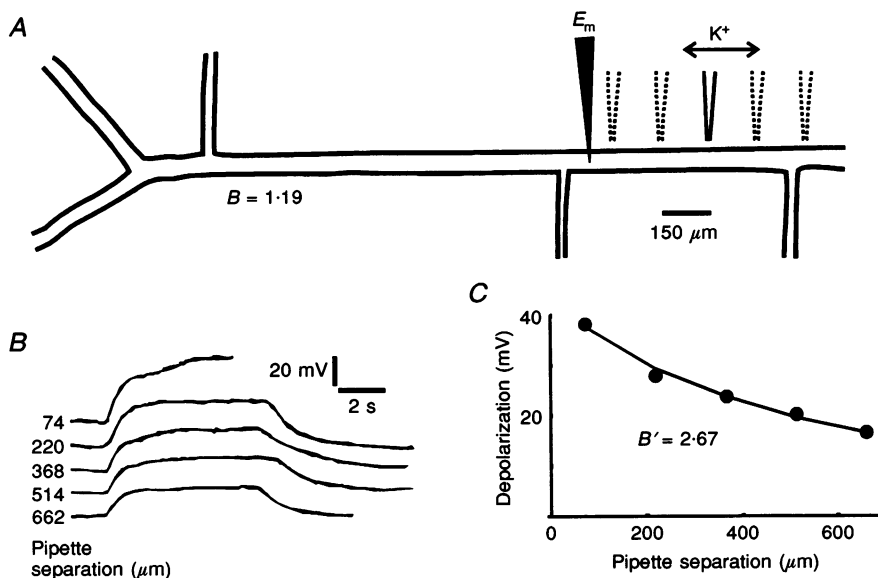
Figure 2. Conducted depolarization in an arteriole network

A, experimental protocol for intracellular recording (filled pipette tip) at a defined site in the arteriole network. A micropipette containing depolarizing (120 mM) K^+ was positioned at ~150 μm increments along the arteriole. *B*, electrical responses recorded when the K^+ pipette was positioned at distances indicated to the left of each record. Last location stimulated was closest to the microelectrode; note secondary plateau in depolarization (not used) prior to the recording electrode being dislodged by constriction of the arteriole. Resting E_m in this cell was −75 mV. *C*, the magnitude of intracellular depolarization (mV) induced by the high-K^+ stimulus at distances indicated in panel *B*. Note the decay of depolarization as the high-K^+ pipette was moved away from the recording site. The small short branch between the two most distant sites of K^+ application appeared to have a negligible effect on the decay of depolarization (compare with Fig. 4), but data from further points were not used in fitting the curve to estimate *B'*.

two reasons. First, in previous experiments in our laboratory the constriction caused by brief applications of the high-K^+ solution was found to be unaffected by 30 nM ω-conotoxin GVIA, suggesting that neurotransmitter release was not involved (Neild & Lewis, 1995). Second, in experiments in which the nerves around these arterioles were stimulated deliberately (Hirst, 1977) the constriction was not local, but spread uniformly for several millimetres throughout the arteriolar tree.

Calculation of the expansion parameter *B*

An estimate (*B'*) of the expansion parameter *B* was calculated by finding the best fit of eqn (A10) (see Appendix) to depolarization amplitudes measured with respect to separation distance. One example is shown in Fig. 2. In all but one case, *B'* was greater than the anatomical *B* for corresponding networks (Fig. 3). This is the direction of error expected if the high-K^+ stimulus caused a fall in membrane resistance or there was leakage of current around the recording electrode (see below).

Figure 3. Relationship between *B* calculated from network anatomy and *B'* estimated from electrophysiological measurements

The two values were significantly correlated ($r = 0.71$, $P < 0.05$), but *B'* tended to overestimate *B* by a factor of ~2.5. Continuous line is the least-squares regression line.
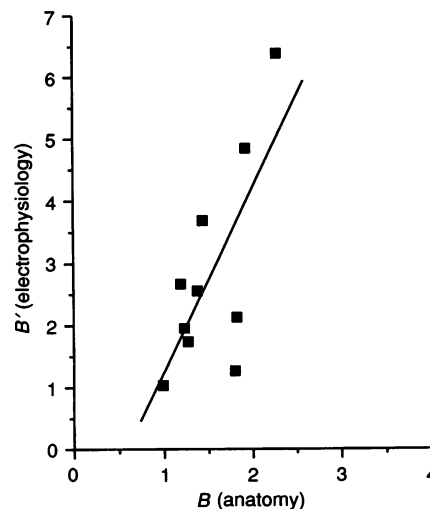
However, as shown in Fig. 3 our estimate, B', was significantly correlated with values of B calculated from the structure of the arteriolar trees. This correspondence shows that both methods were sensitive to differences in architecture (i.e. expansion properties) between networks.

In four experiments there was a branch arteriole within ~500 μm of the recording site. For these cases, additional data were acquired for high-K^+ stimulations at sites beyond the branch, in order to determine the effect of branching on conduction along an otherwise continuous 'cable.' As expected, there was a discontinuity in the depolarization curve at the site of the branch because of the additional path for signal dissipation, as shown in Fig. 4. In such cases, the data acquired for stimuli beyond the branch were not used in the calculation of B'.

Effect of our assumptions on B'

When applying eqn (A10) to our data we assumed that: (i) λ was constant at 1·2 mm, and (ii) the magnitude of the depolarization at the site of the high-K^+ stimulus (V_0) was a constant for any one experiment, with a value calculated to give the best fit to the data. There were two free parameters in the fitting procedure, B' and V_0, and both were varied until the best fit was obtained. In the three experiments in which V_0 was measured directly the value from the curve-fitting procedure agreed closely with the value measured.

We tried a variety of additional analysis procedures (described below) that were designed to compensate for possible deviations from our assumptions, but none improved the fit to the data significantly. We found that the most important factor in any of the analyses was the value of λ, in that changes in λ had a far greater effect on B' than changes in any other parameter. We therefore held λ

constant at 1·2 mm, based on the mean value determined by Hirst & Neild (1978).

Change in membrane resistance. One assumption underlying the equations given in the Appendix is that membrane properties do not change due to E_m or ionic changes. We could not fulfil this condition, as our use of the high-K^+ solution would cause a fall in specific membrane resistance (R_m; Hodgkin & Katz, 1949), and the depolarization might have been large enough to activate voltage-sensitive conductances. Assuming that the majority of the resistance change was confined to a region of constant length in the vicinity of the K^+ pipette, this would be equivalent to a local decrease in λ. The length of the affected region would be constant during an experiment, and could be represented in eqn (A10) as a constant amount added to L. However, introducing this constant as an additional free parameter in the curve-fitting procedure did not improve the fit, and its value was usually determined to be very close to 0.

Assuming a uniform decrease in R_m throughout the region between the pipettes was equivalent to choosing a lower value for λ. This gave values of B' closer to B calculated from network anatomy. When we left λ as a free parameter and fixed B to the value calculated from anatomy we obtained values for λ of between 0·6 and 0·7 mm. These values would indicate a fall in R_m by a factor of around four; a reasonable value for these arterioles in 120 mM K^+ (Hodgkin & Katz, 1949; Hirst & Van Helden, 1982).

Dependence of V_0 on network anatomy. As shown in the Appendix, V_0 depends on the anatomy of the arteriolar tree because the region affected by K^+ must supply current to depolarize the attached network. From the three
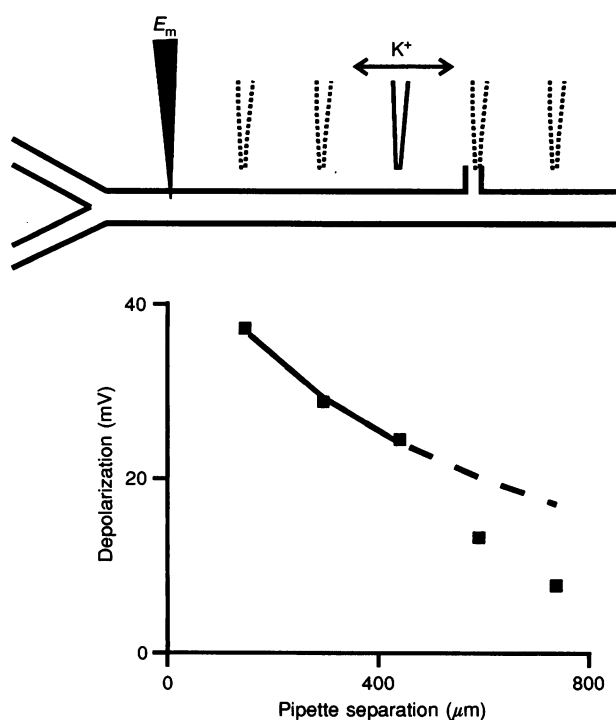
Figure 4. Effect of a branch on conducted depolarization

In this preparation there was a major branch in the region in which K^+ was applied, which resulted in a discontinuity on the plot of depolarization against pipette separation. The smooth curve was fitted to the 3 data points obtained proximal to the branch; the 2 distal points fall below the curve because some current resulting from the distal applications of K^+ flows along the branch.

experiments in which we measured V_0 directly, we verified that it was not equal to the ideal value V_K, the membrane potential that would result if the high-K^+ solution was applied to all the membrane surface. From V_0 and V_K we calculated B_K, a measure of the output resistance of the region depolarized by the K^+, and compared it with B_{in}, the input resistance of the tree expressed in the same way. B_K was greater than B_{in} by a factor of 5·3 on average. We then calculated B' with a more complex model in which V_0 varied with position of the K^+ pipette, taking into account the geometry of the network, and B_K was a free parameter. This procedure did not result in a better fit to the data, and the discrepancy between B and B' was not reduced. B_K was always more than twice B_{in} and usually greater, and the variation in V_0 was around 5 mV (i.e. around 10% of its value), indicating that our initial assumption that V_0 was constant was not unreasonable in practice.

Leakage around the recording electrode. As shown in the Appendix, any leakage around the recording electrode would increase B' by an amount (B_{leak}) that can be estimated from the value of resting E_m recorded. When we assumed that the true value of resting E_m was −80 mV, the mean value of B_{leak} was only 0·023, which was not sufficient to explain the discrepancy between B and B'. If we had assumed a less negative value for the true resting potential, B_{leak} would have been even smaller.

Verification that recordings were made from smooth muscle cells

Our assumption that we were recording E_m from smooth muscle cells (rather than endothelium) was checked by making a series of recordings using microelectrodes filled with the dye Lucifer Yellow. These microelectrodes had higher resistances and less stable tip potentials, making them less suitable for high-quality E_m recordings. Once a cell was penetrated and a stable recording obtained, the dye was microiontophoresed (2–5 nA DC) intracellularly via a current injection circuit in the electrometer. The preparations were fixed and viewed after the experiment; in all six experiments dye was found exclusively in smooth muscle cells (Fig. 5). Dye did not spread to other cells, and was never seen in an endothelial cell. We therefore conclude that all recordings made here were from smooth muscle cells. If endothelial cells were actually recorded from in some cases, response characteristics were not distinguishable, which supports the hypothesis of electrical coupling between cells of the arteriole wall (Rhodin, 1967; Hirst & Neild, 1978; Segal & Duling, 1986, 1989; Segal & Bény, 1992; Bény & Pacicca, 1994; Xia *et al.* 1995).

E_m changes associated with conducted vasoconstriction

In our experiments described above, the depolarizations caused by positioning the high-K^+ pipette at designated sites along the arteriole reached a stable plateau within 2–3 s (Fig. 2); under these conditions the corresponding (sustained) vasoconstriction occurred over a distance of 200–300 μm on either side of the high-K^+ pipette. In experiments on cheek pouch (Segal & Duling, 1986, 1989; Segal *et al.* 1989) and cremaster muscle (Segal, 1991) arterioles, microiontophoretic pulses (250–500 ms) of a vasoconstrictor (e.g. noradrenaline) or vasodilator (acetylcholine) produced diameter responses that spread along arterioles over distances encompassing several millimetres. Furthermore, the magnitude of conducted responses did not change abruptly at branch points (Segal, 1991) as we predict they would if purely passive spread was involved (Figs 4 and 7). Therefore, we varied our experimental conditions in an attempt to achieve similar conduction distances for vasoconstriction in submucosal arterioles. Using pressure
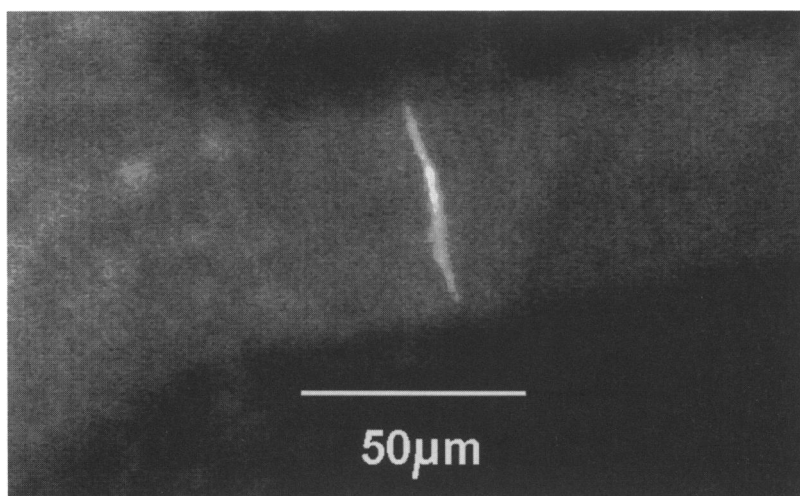
Figure 5. A single smooth muscle cell injected with the fluorescent dye Lucifer Yellow
The cell appears as a bright streak across the full width of the arteriole; in these arterioles most cells are long enough to wrap approximately two-thirds of the way around the vessel (Hua & Cragg, 1980). The outline of the arteriole is faintly visible due to autofluorescence. There was no evidence of dye spreading to other cells in 6 similar experiments.

ejection of high-K⁺ PSS from a micropipette (tip i.d., 5 μm) positioned adjacent to the vessel we were able to induce a more rapid depolarization. This triggered an active response in smooth muscle cells >500 μm from the stimulus site, which was associated with a transient vasoconstriction (Fig. 6). This type of weak regenerative membrane response is common in vascular smooth muscle, being analogous to an action potential (Holman & Surprenant, 1979). The constrictions associated with these active responses spread for more than 1 mm, but further analysis to see if the spread was affected by branching was not possible using our apparatus. Nevertheless, these observations suggest that an active response required a stimulus that caused a rapid depolarization.

DISCUSSION

The influence of arteriolar network geometry on the properties of signal conduction has not previously been considered. Through implementing for the first time a network analysis of the cable properties of signal conduction in arterioles, we have shown that the distance over which a defined stimulus can effect vascular function is diminished as the extent of branching increases. In effect, each arteriole branch acts as an additional 'path' which expands the region over which the signal spreads, thereby contributing to

dissipation of the stimulus. This finding implies that the influence of an electrical event occurring at one location in a network on a cell or branch elsewhere in the network is determined largely by network anatomy and not just the distance between locations.

Network cable properties

Earlier analyses of signal conduction in arterioles have implicitly treated the vessels as continuous unbranched cables (Segal et al. 1989; Segal, 1991; Delashaw & Duling, 1991); branching introduces complications which have been either ignored or avoided in prior studies of conduction in arterioles (Hirst & Neild, 1978; Neild, 1983; Segal et al. 1989). Nevertheless, as we have shown here, it is possible to predict the electrical properties of an arteriolar network from its structure and then compare the prediction with the experimental data. Our values for B, determined with intracellular recording, tended to overestimate those calculated from anatomical measures (Fig. 3). Nevertheless, the agreement between values across networks indicates that the electrical properties of a network can be predicted with reasonable accuracy from anatomical measurements. In effect, the significant correlation between functional and anatomical data (Fig. 3) supports the principle finding of this study, that the branching characteristics of a network are a major determinant of signal dissipation.
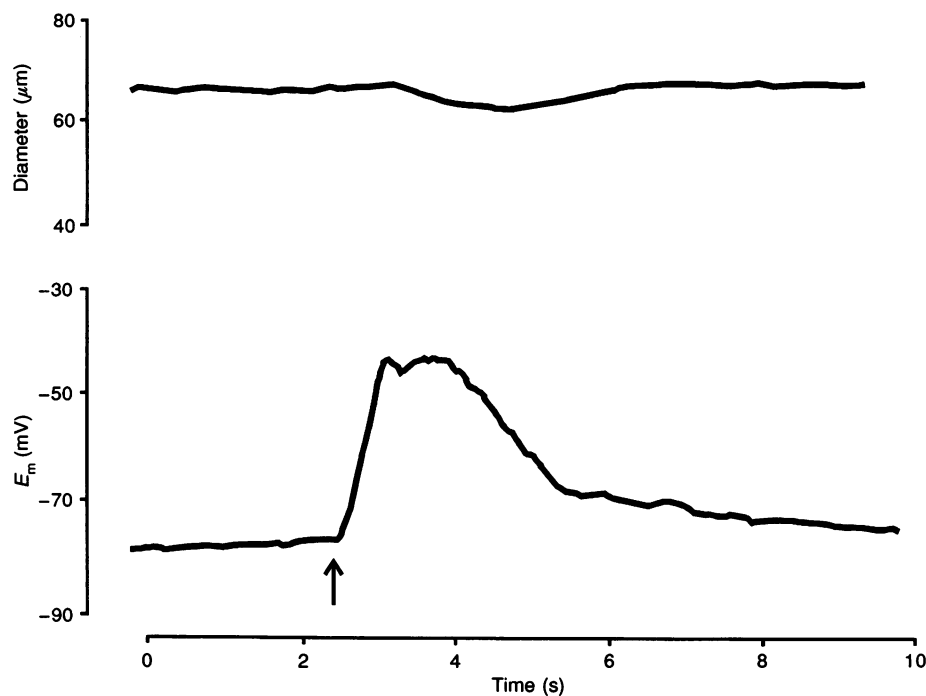
Figure 6. Active electrical response following rapid depolarization

At the time marked by the arrow a pulse (50 lbf in⁻², 1 s) of high-K⁺ solution was ejected from a micropipette (tip i.d., 5 μm) positioned adjacent to the arteriole. Simultaneous recordings of diameter and membrane potential (E_m) were made 550 μm from the stimulus site. Note the rapid onset of depolarization and evidence of an action potential-like event; such rapid peaks were not observed with sustained high-K⁺ stimuli used for calculating B (Fig. 2). The onset of depolarization preceded the start of vasoconstriction by 0·7 s.

The influence of network branching on signal dissipation can be described by the expansion parameter B, which is experimentally derived from anatomical data for a particular network. A simple network consisting of a daughter branch and its parent vessel illustrate the functional significance of these values (Fig. 7). In this example, which represents a situation used in experiments on blood flow control (Segal, 1991), a constant depolarizing stimulus was delivered at the distal end of the daughter branch. The magnitude of depolarization at the vessel origin, located 1λ from the stimulus site ranged from 37% (with $B = 1$) to $\sim$7·5% (with $B = 10$) of its value at the stimulus origin, depending on the relative diameters of the parent and branch arterioles. This calculation assumes passive spread of the E_m change with the membrane electrical properties remaining constant, and applies equally to hyperpolarization.

Conduction of vasomotor responses

The original studies of electrical conduction in arterioles assumed that the smooth muscle cell layer provided the conduction pathway (Hirst & Neild, 1978; Neild, 1983). However, the pronounced dye coupling between arteriolar endothelial cells (Segal & Bény, 1992) implies that they have a key role in transmitting signals along the vessel wall. If endothelial cell and smooth muscle cell layers are electrically coupled (which appears likely), then the analysis of λ in arterioles (Hirst & Neild, 1978; Neild, 1983; Xia *et al.* 1995) must account for both longitudinal and concentric coupling between cell layers. The thickness of the arteriole wall is required for calculating B, and we found that varying it through the range of 2–5 μm caused B to change by <5%. In this context, the inclusion of a 'coupled' endothelial cell layer ($\sim$1 μm thick) in calculating B has little functional significance with respect to the cable properties of arteriole networks.

The 'mechanical length constants' (1·8–2·1 mm) that have been used to describe conducted vasomotor responses (Segal *et al.* 1989; Segal, 1991) are numerically close to λ determined electrophysiologically (1·1–1·6 mm) (Hirst & Neild, 1978), and were based on the assumption that the
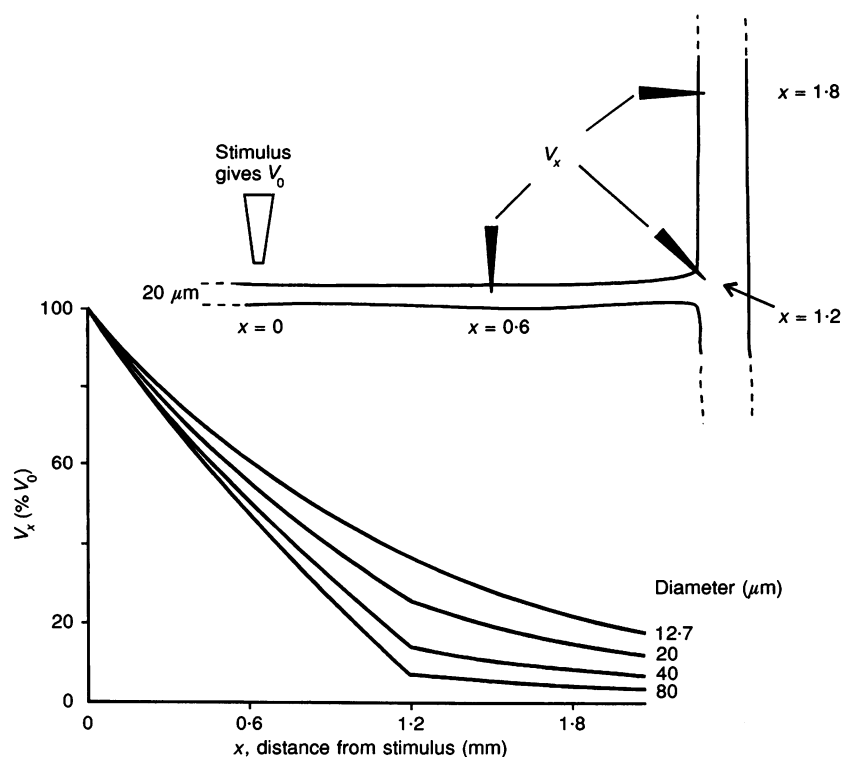
Figure 7. Simulation of the passive decay of E_m change

Simulation of an experiment in which a depolarizing or hyperpolarizing stimulus is applied to a daughter arteriole and the spread of E_m change towards the parent arteriole is measured at the distances indicated. The E_m change at the stimulus site is V_0, and the E_m change V_x at various distances is plotted. The cable space constant λ was set to 1·2 mm. The diameter of the daughter branch was set to 20 μm; response curves are shown for 4 diameters of the parent branch. These diameters (12·7, 20, 40 and 80 μm) correspond to values of B of 1, 2, 4·7 and 10·0 at the branch point. When $B = 1$ (which requires a parent arteriole smaller than the branch) E_m changes decay as in a simple cable, shown in the upper curve. For greater values of B there is a discontinuity in the curves at the distance corresponding to the junction of the two arterioles. The larger the diameter of the parent arteriole relative to the daughter branch, the more rapid the decline of potential change with distance along the branch.

change in diameter reflected a corresponding change in E_m. *In vivo*, however, the influence of branching cannot be overlooked; as shown by the present results, each branch provides an additional path for a signal to spread. Therefore, the range over which a signal (and response) may be conducted *in vivo* is strongly influenced by the network anatomy. The conduction of depolarization that we determined experimentally (and predicted from network geometry) reflects this property, yet rarely is a network encountered in which the electrical signal would be expected to decrement exponentially with a space constant equal to λ. In practice, for data pooled across experiments we found that changes in E_m decayed to $1/e$ (or 37%) in 736 ± 93 μm ($n = 10$; Fig. 8). While these data do not provide an estimate of λ, they illustrate on average the effective distance over which an electrical signal spreads passively in these networks.

The conduction of vasomotor responses has been assumed to reflect the passive spread of electrical signals along the arteriole wall (Segal & Duling, 1986; Segal, 1991). The present findings offer several new perspectives on this assumption. The passive conduction of depolarization in submucosal arterioles dissipates much more rapidly (i.e. over shorter distances) than vasomotor responses in arterioles of the hamster cheek pouch (Segal & Duling, 1986; Segal *et al.* 1989) or cremaster muscle (Segal, 1991). Additionally, our electrophysiological data indicate that the depolarization induced by 120 mM K^+ was conducted over distances that were severalfold greater than for the corresponding vaso-constriction. Two conclusions may be drawn from these observations. First, the passive spread of electrical signals in arteriole networks cannot account for the distances observed for conduction of vasomotor responses. Second,

the original assumption of a direct proportionality between E_m and diameter (Segal *et al.* 1989) is an oversimplification. These shortcomings may be explained in several ways.

From the perspective of electromechanical coupling, a 'threshold' level of depolarization may be required to initiate a vasomotor response. For example, in rat tail arteries exposed to increasing concentrations (5–100 mM) of extracellular KCl, contraction did not occur until smooth muscle cells had depolarized to ~-40 mV (Neild & Kotecha, 1987). Similar behaviour has recently been demonstrated in arteriole segments isolated from the hamster cheek pouch (Xia & Duling, 1995). Applied to the present experiments, the magnitude of depolarization clearly reached threshold in the vicinity of the high-K^+ pipette. However, the decrement in depolarization with distance would have reached a point where smooth muscle cells were insufficiently stimulated to contract. *In vivo*, where vasoconstriction was conducted for > 2 mm along arterioles of the cheek pouch preparation (Segal *et al.* 1989), resting E_m was around -50 mV (Segal & Bény, 1992); i.e. substantially less negative than in submucosal arterioles (typically -70 to -80 mV, Hirst & Van Helden, 1982). This difference in resting E_m is also consistent with a higher resting tone of arterioles *in vivo* when compared with isolated preparations (Xia & Duling, 1995; present data). Against such different baselines, the more negative E_m in intestinal arterioles should depress the effective distance for eliciting vasoconstriction with a given depolarizing stimulus. As shown here, such an effect is augmented in a network: additional paths (i.e. greater dissipation) for conduction would result in relatively less of an arteriole segment (or network) reaching 'threshold' for electromechanical coupling.
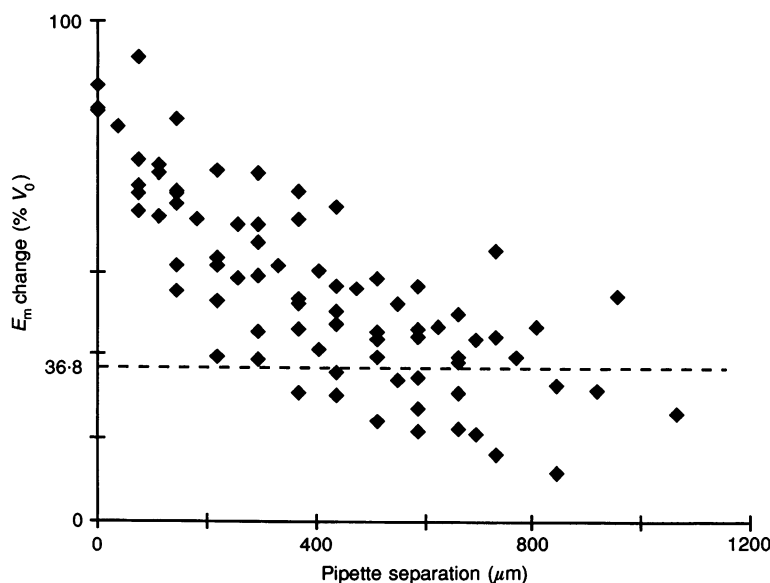

Figure 8. Observed decay of E_m change with distance from the high-K^+ stimulus
Pooled data from 10 experiments. E_m changes are expressed as a percentage of V_0 to allow comparison between data from different experiments. The E_m change decays to $1/e$ (36·8%; dashed line) of its initial value in about 700 μm, but in these branching networks this does not give a measure of λ.

Lastly, studies of conducted vasodilatation and vaso-constriction have relied primarily upon receptor activation to trigger conduction (Segal *et al.* 1989; Delashaw & Duling, 1991), and the activation of receptors can trigger both pharmacomechanical and electromechanical responses via corresponding receptor subtypes (Somlyo *et al.* 1988; Hirst & Edwards, 1989). Whereas conduction has been attributed to the spread of electrical events, receptor occupation may result in additional active components that may not be elicited with a purely depolarizing stimulus as used here. Clearly, there are several fundamental questions that remain to be addressed, each of which will require further experimentation. The channels underlying the active responses, such as shown in Fig. 6, need to be identified. Recordings of E_m during conduction of hyperpolarizing vasodilator responses are also needed, as our results imply that they must be associated with regenerative activity of some kind. It may be due to voltage-sensitive K^+ channels, which can produce regenerative responses resembling an inverted action potential (George & Johnson, 1961).

Critique of methods

In the hamster cheek pouch, dye microinjection while recording from arteriolar endothelial cells or smooth muscle cells *in vivo* (Segal & Bény, 1992) has graphically illustrated that it is invalid to assume that all intracellular recordings from arterioles represent the smooth muscle layer (Hirst & Neild, 1978). Therefore, we performed a series of recordings during which we marked the cells from which we recorded E_m. In these experiments ($n = 6$), each cell that we labelled and recorded from was a smooth muscle cell. In additional experiments, we were unsuccessful in our attempt to impale endothelial cells even when working at the edge of the vessel, where the 'fold' in the wall should increase the chance of impalement. As observed previously (Segal & Bény, 1992), Lucifer Yellow dye was retained within the injected muscle cell (Fig. 5). However, dye coupling need not correlate with electrical coupling (Veenstra *et al.* 1995; Ransom & Kettenmann, 1990). Differences in the charge and structure of dyes (Little *et al.* 1995) and in the connexin protein composition of gap junctions (Veenstra *et al.* 1995) may exclude dye molecules from channels that are readily permeable to small ions and which enable electrical coupling.

There are several key differences between *in vivo* hamster cheek pouch and *in vitro* guinea-pig submucosal preparations for studying arterioles; these differences may contribute to the more negative E_m in mucosal arterioles discussed above. The pouch remains connected to and perfused by the animal, whereas submucosal preparations are isolated. Thus, in the pouch, blood pressure inflates the vessels and thereby maintains the vessel lumen; arterioles have high resting tone and remain functional in controlling blood flow (Segal & Bény, 1992). Recent evidence suggests that transmural pressure *per se* contributes to the manifestation of conducted responses (Lin & Duling, 1994); however, the nature of this relationship has not been

defined. In contrast, arterioles in the intestinal submucosa preparation were studied here while deflated, relaxed and imbedded in a tissue which has been pinned as a taut sheet; these conditions apparently result in an endothelial cell layer that is simply too thin (e.g. $< 1\ \mu m$) to penetrate. Nevertheless, these *in vitro* preparations enable electrical analyses of arteriole trees independent of pressure, flow and humoral factors, all of which are known to influence the E_m and vasomotor activity of smooth muscle and/or endothelial cells (Olesen, Clapham & Davies, 1988; Davis, Donovitz & Hood, 1992; Segal, 1994).

Summary and conclusion

The present study is the first to evaluate arteriole networks as branching cables for the conduction of electrical signals. We have found that as branching of a network increases, there is greater dissipation of a depolarization gradient which can be quantified by the expansion parameter B. This conclusion is substantiated by our finding that such electrophysiological behaviour was correlated with (and therefore could be predicted from) the underlying network anatomy. These results imply that the response of an arteriole branch or an individual cell in a network to an electrical event originating elsewhere in the network is determined largely by network anatomy and not simply by the distance between the two sites. Nevertheless, the present results cannot account for the conduction of vaso-motor responses over distances which are severalfold greater than observed here for the passive spread of electrical signals, and point to the need for regenerative activity analogous to an action potential. Therefore, in spite of considerable evidence that cell-to-cell coupling is the basis of conduction, we do not yet fully understand how information is transferred along the arteriolar wall to effect responses at locations further removed from the stimulus site. It is clear that the original assumption of a correspondence between changes in E_m and diameter (Segal *et al.* 1989) requires modification. In turn, this conclusion points to the need for greater understanding of the relationship between E_m and diameter and of the signal transduction pathways which underlie the conduction of vasomotor responses.

APPENDIX

by Timothy O. Neild

Cable properties of hollow cylindrical structures

Hollow cylinders of electrically conducting tissue such as arterioles behave as linear cables (Hirst & Neild, 1978). However, the relationship between their cable properties and basic membrane and cytoplasmic properties is not the same as it is for the better-known case of a solid cylinder, such as a nerve axon. A simple electrical equivalent of an arteriole whose wall consists of electrically coupled cells is a hollow cylinder of conducting cytoplasm bounded on the outer and inner (luminal) surface by a poorly conducting membrane (Fig. A1).
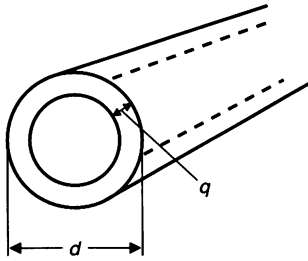
Figure A1. A hollow cylinder, electrically equivalent to an arteriole

The inner and outer walls of the cylinder are poorly conducting, and correspond to the membranes of the cells in the wall. The substance between the walls has a lower resistance determined by the cytoplasmic resistivity and the coupling resistances between the cells. The lumen is assumed to be connected to the extracellular space, both of which contain a conducting fluid of low resistivity.

If the outer diameter is d, and the thickness of the wall is q, the perimeter of a transverse section of the cylindrical cable is given by:

$$\pi d + \pi(d - 2q) = 2\pi(d - q), \tag{A1}$$

thus the cable membrane resistance per unit length for an infinite parallel cylinder is:

$$r_m = \frac{R_m}{2\pi(d - q)}, \tag{A2}$$

where R_m is the specific membrane resistance. Similarly, the area of cross-section is given by:

$$\pi(d/2)^2 - \pi(d/2 - q)^2 = q\pi(d - q), \tag{A3}$$

and the cable resistance per unit length by:

$$r_a = \frac{R_i}{q\pi(d - q)}, \tag{A4}$$

where R_i is the resistivity of the cytoplasm. The space constant is given by:

$$\lambda = \sqrt{\left(\frac{r_m}{r_a}\right)} = \sqrt{\left(\frac{R_m q\pi(d - q)}{R_i 2\pi(d - q)}\right)} = \sqrt{\left(\frac{R_m q}{R_i 2}\right)}. \tag{A5}$$

The space constant is independent of arteriole diameter, in contrast to a solid cylinder such as an axon. This greatly simplifies the analysis of branching arteriolar networks described below.

The input resistance of an infinite hollow cylinder is given by:

$$R_{in} = \frac{\sqrt{(r_m r_a)}}{2} = \frac{1}{2\pi(d - q)}\sqrt{\left(\frac{R_m R_i}{2q}\right)}. \tag{A6}$$

Input resistance is inversely proportional to $(d - q)$; again, this is different from a solid cylinder, where input resistance varies as $1/d^{3/2}$.

Setting $q = d/2$, a limiting case equivalent to a wall so thick that there is no lumen, in eqns (A2), (A4), (A5) and (A6)

gives the equivalent expressions that apply to a solid cylinder or cable (Jack et al. 1975; chap. 3).

Analysis of branching networks

The spread of membrane potential (E_m) changes in the branching dendrites of neurones has been studied by several workers, and their results can be applied to branching arteriolar trees with very little modification. A summary is given by Jack et al. (1975; chap. 7), which also includes the derivations of the equations and references to other original work.

An unbranched segment of an arteriolar tree can be represented as a single cylindrical structure, as in Fig. A2. If an applied current causes an E_m change of V_0 at one point, the E_m change V_X recorded at a distance X is given by:

$$V_X = V_0 \frac{\cosh(L - X) + B\sinh(L - X)}{\cosh(L) + B\sinh(L)}, \tag{A7}$$

where L is the length of the segment up to the point at which it branches or changes diameter. L is given by l/λ, where l is the separation measured in real units, and λ is the space constant expressed in the same units. Similarly, X is given by x/λ, where x is the distance in real units.

B in eqn (A7) is the parameter that describes the effect of the branching or other structural change. One way to interpret B is in terms of the input conductance of the network beyond the recording electrode. If the arteriole continues on to infinity without branching or diameter change its input conductance is G_∞ ($= 1/(2R_{in})$). If its structure is in some way different from an infinite parallel cable, its input conductance is defined as $G_\infty B$, i.e. B is the factor by which input conductance differs from that of an infinite cable. Branching or expanding cable networks require $B > 1$; sealed ends of a terminated cable have $B = 0$.

B depends on the lengths and relative diameters of the branches in a network, and it can be calculated from anatomical data if the space constant of the conducting
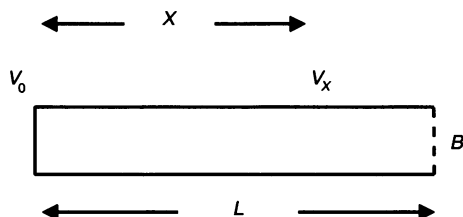
Figure A2. Diagram to show the terminology used to describe E_m changes in a segment of arteriolar tree

If a segment of arteriole length L has its E_m changed to V_0 at one end, the E_m at distance X will be V_X. It will depend partly on B at the end opposite to the stimulus.
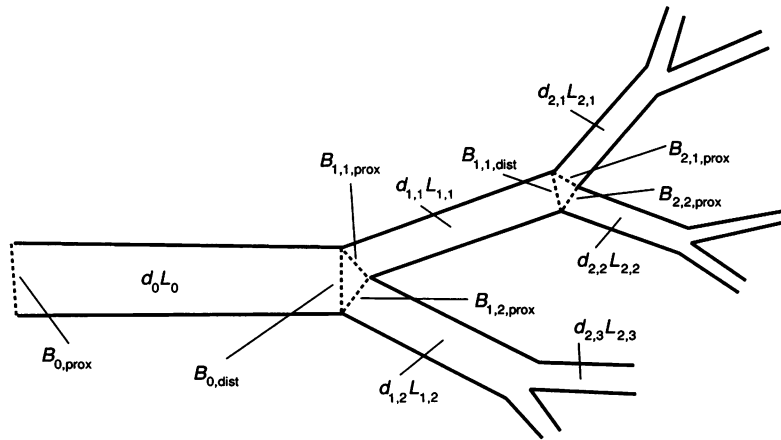
Figure A3. Definition of terms used to describe a branching tree

Every segment of the arteriolar tree has a diameter d and a length L. In the calculations two values of B are defined for each segment, one for each end of the segment. In our experiments we have taken the point of stimulus (K^+ application) as our reference and defined proximal B_{prox} and distal B_{dist} terms for each segment accordingly. (In our experiments this always corresponded to proximal and distal with respect to blood flow from the heart, but this is coincidental and not required for our analysis.) Branches are identified by the 2 numerical subscripts: the first is the branch order and the second identifies the individual branch within the order.

tissue is known. The methods were worked out for the dendritic trees of neurones (Jack *et al.* 1975), but require only slight modification for vascular networks.

The network must first be represented as a binary branching tree as shown in Fig. A3. At any point in this network a value of B can be defined that summarizes the input conductance of more distal parts of the network. For each segment of the tree it is convenient to define two values of B, B_{prox} and B_{dist}. B as discussed above is B_{dist}, which summarizes the properties of the network distal to the branch under consideration. B_{prox} is the equivalent parameter required when considering voltage changes at the proximal end of the segment, and takes into account the properties of the segment itself. At a branch point, B_{dist} for the parent is the sum of the B_{prox} values for the individual branches scaled to take into account the relative diameters (d) of the branch and the parent vessel to which it connects. For the example shown in Fig. A3:

$$B_{0,\mathrm{dist}} = B_{1,1,\mathrm{prox}}\frac{(d_{1,1} - q)}{(d_0 - q)} + B_{1,2,\mathrm{prox}}\frac{(d_{1,2} - q)}{(d_0 - q)}. \quad (A8)$$

The values $B_{1,1,\mathrm{prox}}$ and $B_{1,2,\mathrm{prox}}$ required to evaluate this expression are found from the length of the branch distal to

them and the B_{dist} for the network attached to its far end. For example:

$$B_{1,1,\mathrm{prox}} = \frac{B_{1,1,\mathrm{dist}} + \tanh(L_{1,1})}{1 + B_{1,1,\mathrm{dist}}\tanh(L_{1,1})}, \quad (A9)$$

where $L_{1,1}$ is the normalized length of the branch, $l_{1,1}/\lambda$.

There are two important differences between these expressions and those derived for dendritic trees of solid rather than hollow structures. In dendrites the space constant depends on diameter, and a 'local' space constant must be used for each branch. In hollow cylinders the space constant is independent of diameter (eqn (A5)), and so the same value of space constant applies in all expressions, provided membrane properties and wall thickness remain the same. There is also a different relationship between input resistance and diameter (eqn (A6)), such that eqn (A8) contains a ratio of ($d - q$), whereas the equivalent equation for dendrites contains a ratio of diameters raised to the power 3/2.

Our experimental situation is shown diagrammatically in Fig. A4. We recorded smooth muscle E_m from one point in a branching network with a parallel unbranched region of arteriole to the left of the recording site and a branching
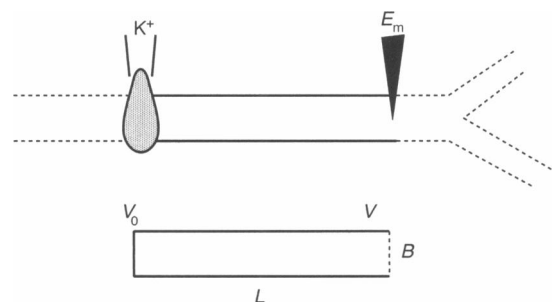
Figure A4. Relationship between the experiment and the formal description of the arteriolar segment

A

B

$V_K = 0$ mV
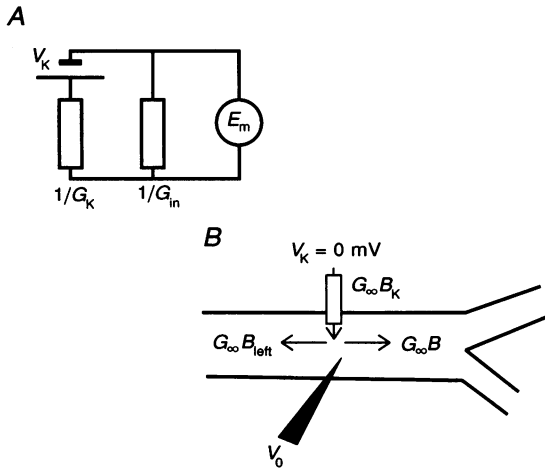
Figure A5. Factors determining the depolarization produced by external K^+ application

A, equivalent circuit of the cells in the arteriole wall in the region where 120 mM K^+ is applied. The E_m is dependent on the K^+ equilibrium potential V_K and the input total conductance of the arteriolar network G_{in}. An additional conductance G_K is used to allow for the limited ability of the depolarized region to supply current to the rest of the network; it represents the output conductance of the depolarized region. *B*, representation of the experimental situation, in which application causes an E_m change (V_0) at the point of application. The conductances represented in *A* have been expressed in terms of G_∞ and their own particular *B* values, as in eqn (A11).

network to the right. A concentration of 120 mM K^+ was applied to regions of the arteriole to the left of the recording site to impose a repeatable E_m change at the point of application. In the simplest case, this stimulus imposes a new level of E_m, V_0, on the tissue; it is not a constant current stimulus. The structure of the vascular tree to the left of the K^+ application then has no effect on the E_m change to the right.

The region of arteriole between the K^+ pipette and the recording electrode can therefore be treated as a finite cable-like structure. At the left end, K^+ application imposes a depolarization, V_0, of unknown amplitude; at the right end we record an attenuated depolarization V that depends on the properties of the cable, the separation between the stimulating and recording pipettes, and the nature of the termination at the right end. The E_m change (V) that we record is related to the change V_0 imposed by the high-K^+ by:

$$V = V_0\left(\frac{1}{(\cosh L + B\sinh L)}\right),\qquad (A10)$$

where L is the normalized separation between the K^+ pipette and the recording site, and B is B_{dist} for the segment from which the recording is made.

Assumptions concerning the value of V_0

If the whole arteriolar preparation was exposed to the 120 mM K^+ solution contained in our high-K^+ pipette, the E_m would have a value close to 0 mV (Hirst & Van Helden, 1982). When the high-K^+ solution was applied to a restricted region, the E_m change (V_0) that occurred depended on the ability of that region to supply current to the rest of the arteriolar tree (i.e. the 'output resistance' of the depolarized region).

The equivalent circuit is shown in Fig. A5*A*, where E_m is the membrane potential and V_K is the membrane potential that would result if the high-K^+ solution was applied to all the membrane surface. The value of E_m depends on two resistances; $1/G_{in}$, which is the input resistance of the arteriolar network and $1/G_K$, the 'output resistance' of the region depolarized by the high-K^+ solution. In Fig. A5*B* the arteriole is represented to show that G_{in} is the sum of two components, $G_\infty B$ and $G_\infty B_{left}$, which depend on the arteriolar geometry. The output resistance of the depolarized section can also be expressed in this way with the introduction of B_K to describe its properties. If B_K is large relative to $B + B_{left}$, then V_0 will be close to V_K and practically independent of arteriolar geometry. For lower

A

B
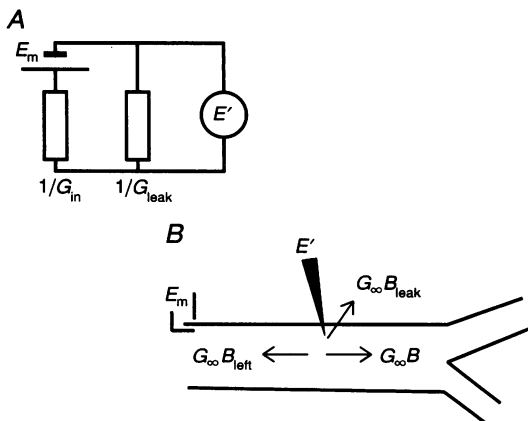
Figure A6. Effect of leakage around the recording electrode

A, equivalent circuit of the cells in the arteriole wall at the point of intracellular recording of membrane potential. The potential recorded (E') is determined by the true membrane potential E_m, the input conductance of the arteriolar network G_{in}, and the leakage conductance around the recording electrode G_{leak}. *B*, representation of the experimental situation. The conductances represented in *A* have been expressed in terms of G_∞ and their own particular *B* values, as in eqn (A12).

values of B_K, V_0 will be influenced to some extent by the structure of the arteriolar tree.

$$V_0 = V_K\left(\frac{1/G_{in}}{1/G_K + 1/G_{in}}\right)$$

$$= V_K\left(\frac{1/B_{left} + 1/B}{1/B_K + (1/B_{left} + 1/B)}\right). \qquad (A11)$$

Leakage around the intracellular microelectrode

If there is any leakage around the intracellular recording electrode, it will provide an additional current pathway, which in our experiments could not be distinguished from the pathway into the branching network. This would lead to an overestimate of B. However, if the true value of the resting potential is known, the possible error in B can be estimated from the value of the resting potential actually recorded.

Leakage around an intracellular microelectrode leads to an error in E', the E_m recorded, compared with the true value E_m.

The leakage conductance around the electrode (Fig. A6) is G_{leak} and the total transmembrane conductance apparent from the recording site is G_m. As above, these can be re-expressed in terms of G_∞ and appropriate B values:

$$E' = E_m\left(\frac{1/G_{leak}}{1/G_{leak} + 1/G_m}\right)$$

$$= E_m\left(\frac{1/B_{leak}}{1/B_{leak} + (1/B_{left} + 1/B)}\right). \qquad (A12)$$

As both B and B_{left} can be estimated from measurements of the structure of the network using eqns (A8) and (A9), B_{leak} can be calculated if a reliable value for E_m, the true resting potential, is available.

BÉNY, J.-L. & PACICCA, C. (1994). Bidirectional electrical communication between smooth muscle and endothelial cells in the pig coronary artery. *American Journal of Physiology* **266**, H1465–1472.

CHEN, G. & CHEUNG, D. (1992). Characterization of acetylcholine induced membrane hyperpolarization in endothelial cells. *Circulation Research* **70**, 257–263.

DAVIS, M. J., DONOVITZ, J. A. & HOOD, J. D. (1992). Stretch-activated single channel and whole cell currents in vascular smooth muscle cells. *American Journal of Physiology* **262**, C1083–1088.

DELASHAW, J. B. & DULING, B. R. (1991). Heterogeneity in conducted arteriolar vasomotor response is agonist dependent. *American Journal of Physiology* **260**, H1276–1282.

DULING, B. R. & BERNE, R. M. (1970). Propagated vasodilation in the microcirculation of the hamster cheek pouch. *Circulation Research* **26**, 163–170.

GEORGE, E. P. & JOHNSON, E. A. (1961). Solutions of the Hodgkin–Huxley equations for squid axon treated with tetra-ethylammonium and in potassium-rich media. *Australian Journal of Experimental Biology and Medical Science* **39**, 275–294.

HIRST, G. D. S. (1977). Neuromuscular transmission in the guinea-pig submucosa. *Journal of Physiology* **273**, 263–275.

HIRST, G. D. S. & EDWARDS, F. R. (1989). Sympathetic neuroeffector transmission in arteries and arterioles. *Physiological Reviews* **69**, 546–604.

HIRST, G. D. S. & NEILD, T. O. (1978). An analysis of excitatory junctional potentials recorded from arterioles. *Journal of Physiology* **80**, 87–104.

HIRST, G. D. S. & VAN HELDEN, D. F. (1982). Ionic basis of the resting potential of submucosal arterioles of the ileum of the guinea-pig. *Journal of Physiology* **333**, 53–67.

HODGKIN, A. L. & KATZ, B. (1949). The effect of sodium ions on the electrical activity of the giant axon of the squid. *Journal of Physiology* **108**, 37–77.

HOLMAN, M. E. & SURPRENANT, A. (1979). Some properties of the excitatory junction potentials recorded from saphenous arteries of rabbits. *Journal of Physiology* **287**, 337–351.

HUA, C. & CRAGG, B. (1980). Measurements of smooth muscle cells in arterioles of guinea-pig ileum. *Acta Anatomica* **107**, 224–230.

JACK, J. J. B., NOBLE, D. & TSIEN, R. W. (1975). Mathematical models of the nerve cell. In *Electric Current Flow in Excitable Cells*, ed. JACK, J. J. B., NOBLE, D. & TSIEN, R. W., pp. 131–147. Clarendon Press, Oxford, UK.

KROGH, A., HARROP, G. A. & REHBERG, P. B. (1922). Studies on the physiology of capillaries. III. The innervation of the blood vessels in the hind legs of the frog. *Journal of Physiology* **56**, 179–189.

KURJIAKA, D. T. & SEGAL, S. S. (1995). Conducted vasodilation elevates flow in arteriole networks of hamster striated muscle. *American Journal of Physiology* **269**, H1723–1728.

LIN, Y. & DULING, B. R. (1994). Vulnerability of conducted vasomotor response to ischemia. *American Journal of Physiology* **267**, H2363–2370.

LITTLE, T. L., XIA, J. & DULING, B. R. (1995). Dye tracers define differential endothelial and smooth muscle coupling patterns within the arteriolar wall. *Circulation Research* **76**, 498–504.

MORGAN, K. G. (1983). Electrophysiological differentiation of α-receptors on arteriolar smooth muscle. *American Journal of Physiology* **244**, H540–545.

NEILD, T. O. (1983). The relation between the structure and innervation of small arteries and arterioles and the smooth muscle membrane potential changes expected at different levels of sympathetic nerve activity. *Proceedings of the Royal Society* B **220**, 237–249.

NEILD, T. O. & KOTECHA, N. (1987). Relation between membrane potential and contractile force in smooth muscle of the rat tail artery during stimulation by norepinephrine, 5-hydroxytryptamine and potassium. *Circulation Research* **60**, 791–795.

NEILD, T. O. & LEWIS, C. J. (1995). Reduction of vasoconstriction mediated by neuropeptide Y Y_2 receptors in arterioles of the guinea-pig small intestine. *British Journal of Pharmacology* **115**, 220–221.

OLESEN, S. P., CLAPHAM, D. & DAVIES, P. F. (1988). Haemodynamic shear stress activates a K^+ current in vascular endothelial cells. *Nature* **331**, 168–170.

OLESEN, S. P., DAVIES, P. F. & CLAPHAM, D. (1988). Muscarinic activated K^+ current in bovine aortic endothelial cells. *Circulation Research* **62**, 1059–1064.

RANSOM, B. & KETTENMANN, H. (1990). Electrical coupling, without dye coupling, between mammalian astrocytes and oligodendrocytes in cell culture. *Glia* **3**, 258–266.

RHODIN, J. A. G. (1967). The ultrastructure of mammalian arterioles and precapillary sphincters. *Journal of Ultrastructure Research* **18**, 181–223.

SEGAL, S. S. (1991). Microvascular recruitment in hamster striated muscle: role for conducted vasodilation. *American Journal of Physiology* **261**, H181–189.

SEGAL, S. S. (1994). Cell-to-cell communication coordinates blood flow control. *Hypertension* (Dallas) **23**, 1113–1120.

SEGAL, S. S. & BÉNY, J. L. (1992). Intracellular recording and dye transfer in arterioles during blood flow control. *American Journal of Physiology* **263**, H1–7.

SEGAL, S. S., DAMON, D. N. & DULING, B. R. (1989). Propagation of vasomotor responses coordinates arteriolar resistances. *American Journal of Physiology* **256**, H832–837.

SEGAL, S. S. & DULING, B. R. (1986). Flow control among microvessels coordinated by intercellular conduction. *Science* **234**, 868–870.

SEGAL, S. S. & DULING, B. R. (1989). Conduction of vasomotor responses in arterioles: a role for cell-to-cell coupling? *American Journal of Physiology* **256**, H838–845.

SOMLYO, A. P., WALKER, J. W., GOLDMAN, Y. E., TRENTHAM, D. R., KOBAYASHI, S., KITAZAWA, T. & SOMLYO, A. V. (1988). Inositol trisphosphate, calcium and muscle contraction. *Philosophical Transactions of the Royal Society* B **320**, 399–414.

VEENSTRA, R. D., WANG, H-Z., BEBLO, D. A., CHILTON, M. G., HARRIS, A. L., BEYER, E. C. & BRINK, P. R. (1995). Selectivity of connexin-specific gap junctions does not correlate with channel conductance. *Circulation Research* **77**, 1156–1165.

XIA, J. & DULING, B. R. (1995). Electromechanical coupling and the conducted vasomotor response. *American Journal of Physiology* **269**, H2022–2030.

XIA, J., LITTLE, T. L. & DULING, B. R. (1995). Cellular pathways of the conducted electrical response in arterioles of hamster cheek pouch *in vitro*. *American Journal of Physiology* **269**, H2031–2038.

Author's email address

S. S. Segal: SSSegal@aol.com